Structure–activity relationship of novel DAPK inhibitors identified by structure-based virtual screening

Masako Okamoto [a,*], Kiyoshi Takayama [b], Tomoko Shimizu [b], Ayumu Muroya [a], Toshio Furuya [a]

[a] Drug Discovery Department, Research & Development Division, PharmaDesign, Inc., 2-19-8 Hatchobori, Chuo-ku, Tokyo 104-0032, Japan
[b] NB Health Laboratory Co. Ltd, A1-551 12-18, Kamioki 3, Kawaguchi City, Saitama 333-0844, Japan

ABSTRACT

Death-associated protein kinase (DAPK) is a serine/threonine protein kinase implicated in diverse programmed cell death pathways. DAPK is a promising target protein for the treatment of ischemic diseases. We identified novel potent and selective DAPK inhibitors efficiently by structure-based virtual screening, then further developed the hit compounds. In this paper, we describe the development of the hit compounds and the structure–activity relationship studies of the DAPK inhibitors in detail, including calculation of the solvated interaction energy (SIE), and verification of selectivity using a kinase panel.

© 2010 Elsevier Ltd. All rights reserved.

1. Introduction

DAP-kinase (DAPK), a Ca^{2+}/calmodulin activated Ser/Thr kinase, was originally identified by Adi Kimchi and co-workers at the Weizmann Institute while screening for genes critical for IFN-γ-induced cell death.[1] DAPK belongs to a family of related death kinases, all of which share significant sequence and functional homology. This family includes two closely related homologues of DAPK (DAPK1): ZIPK [ZIP kinase, also known as Dlk (DAP-like kinase) or DAPK3] and DRP-1 (DAPK-related protein 1, also known as DAPK2). There are two other protein kinases which display homology to DAPK: DRAK-1 and DRAK-2 (DAPK-related apoptosis-inducing protein kinase-1 and -2), although these are more distantly related[2] and have been less well characterized.

DAPK is necessary for the regulation or execution of cell death in response to various stimuli, including death receptor activation, cytokines, matrix detachment, ceramide,[3] and others. DAPK is linked to both type I apoptotic and type II autophagic cell death in both caspase-dependent and caspase-independent manners.[2]

Shamloo et al. showed that DAPK plays an important role in ischemic rat brain injuries. They characterized the mechanisms of DAPK activation during ischemia and showed that DAPK is dephosphorylated and activated following ischemia in the brain. Based on their findings, Shamloo et al. suggested that DAPK could be a good therapeutic target for treating acute ischemic stroke.[4]

Inhibition of DAPK would likely intercept cell death and prevent further damage of ischemic regions in cerebral infarction and other ischemic diseases. Interestingly, Velentza et al. reported that a single intraperitoneal injection of a DAPK non-selective inhibitor, an alkylated 3-amino-6-phenylpyridazine, reduced in vivo brain injury in an animal model when administered 6 h after the insult, which is the minimal desired therapeutic time window.[5] Although there have been only a few detailed studies of DAPK as a drug target, it would be useful to have more potent and selective inhibitors against DAPK in order to determine their possible application to unmet needs.

We have previously reported DAPK inhibitors discovered through our structure-based virtual screening (SBVS) research program.[6] In this paper, we describe the general protocol of our in silico approach, and the strategy used to develop hit compounds. In addition, the studies conducted on the structure–activity relationship (SAR) of DAPK inhibitors are discussed in detail.

2. Results and discussion

2.1. Structure-based virtual screening

The general protocol of our in silico approach using structure-based virtual screening is shown in Figure 1. First, for more efficient virtual screening, we typically use several hundreds of thousands of compounds that have been refined using drug-likeness filtering and clustering from commercially available compound databases.[7] Second, we generate protein–ligand complex models using MultiCopyMD,[6,8] an in-house molecular dynamics simula-

---

* Corresponding author. Tel.: +81 3 3523 9630; fax: +81 3 3523 9631.
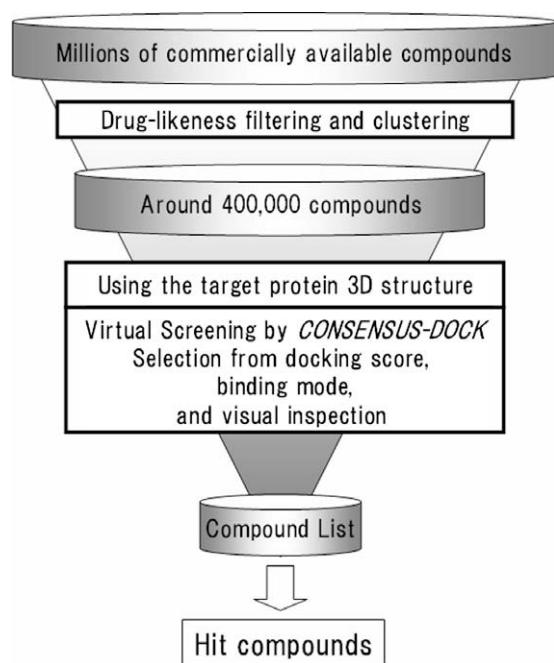*E-mail address:* okamoto@pharmadesign.co.jp (M. Okamoto).

Figure 1. Outline of our in silico approach.

tion program. Third, using the model protein structure, we carry out virtual screening using CONSENSUS-DOCK,[6] an in-house docking calculation program. As reported previously in detail,[6] we make a compound list which includes hundreds of compounds. Kinase inhibition assays were conducted for 100 compounds in the selected compound list, resulting in the identification of four hit compounds.[6] One of these compounds, compound **1**, is shown in Table 1.

2.2. Strategy for the development of hit compounds

After identifying the first hit compounds by virtual screening, we carried out a similarity search using these hit compounds as queries against commercially available compound databases. Compounds were selected for the second screening by their similarity calculated fingerprint based on the descriptors of the BIT_MACCS and visual inspection. The results of kinase inhibition assays conducted on the selected compounds are shown in Table 1.

We predicted the binding mode using docking calculation results and considered SAR of the active compounds from the second screening in choosing the core scaffold for the design of compounds with inhibitory activity. Using the core scaffold as a query, a substructure search was carried out against commercially available compound databases, leading to the selection of compounds for the third screening. The results of the kinase inhibition assay for these selected compounds (third screening) are shown in Tables 2 and 3. This process resulted in the selection of potent and selective DAPK inhibitors.

2.3. Similarity search and substructure search

2.3.1. Similarity search

The first hit compound (compound **1**) and active compounds from the second screening (compounds **2–10**) are shown in Table 1. Compound **2** differed from compound **1** in that the pyridinyl group was replaced with a phenyl group. The inhibitory activity of compound **2** was significantly decreased, suggesting that the pyridinyl group is essential for DAPK inhibitory activity in this ser-

ies of compounds. Compound **5** contained a lactone ring and had much lower inhibitory activity compared to compound **9**, which had an oxazolone ring. Compound **4** contained a thiazolone ring and had modest inhibitory activity. Taken together, these results suggest that the oxazolone ring is essential for potent inhibitory activity.

As shown in Table 1, compounds containing a pyridinyl group, oxazolone ring and phenyl ring (compounds **1**, **6**, **7**, **8**, **9**, **10**) indicated more potent activity than compounds lacking one or more of these rings (compounds **2**, **3**, **4**, **5**). It therefore appears that in this family of compounds, the pyridinyl group, oxazolone ring and phenyl ring are very important for potent DAPK inhibitory activity.

Compound **1** was docked into the ATP binding site of the protein–ligand complex model built by MultiCopyMD[6] using the in-house docking program CONSENSUS-DOCK.[6] As shown in Figure 2, for this binding mode for compound **1**, a hydrogen bond is formed between the nitrogen atom in the pyridinyl group and the backbone NH of Val96 in the hinge region, and some vacancy around the phenyl group is observed. This predicted binding mode suggested that optimization might require substitution of the phenyl ring. Therefore, the third screening was conducted using the chosen core scaffolds as queries and three variable components: a pyridinyl group, an oxazolone ring, and a phenyl ring (shown above Tables 2 and 3).
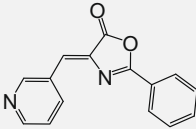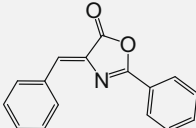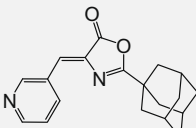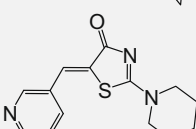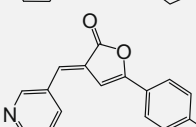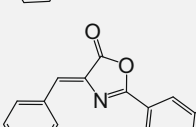
2.3.2. Substructure search

We conducted a substructure search against commercially available compound databases using two core scaffolds as queries: 2-phenyl-4-(3-pyridinylmethylene)-5(4*H*)-oxazolone (Scaffold I) and 2-phenyl-4-(4-pyridinylmethylene)-5(4*H*)-oxazolone (Scaffold II). The results of the query of Scaffold I and Scaffold II are shown in Tables 2 and 3, respectively. Note that the kinase inhibition assay results using compounds with various substituted groups (R_1–R_5) were conducted at 10 μM and 1 μM in Tables 2 and 3.

As shown in Table 2, many phenyl ring substituted derivatives appeared to have more potent inhibitory activity than compound **1** (first hit compound). Nine compounds (compounds **7**, **9**, **11**, **12**, **13**, **15**, **17**, **18**, **21**) retained potent inhibitory activity even at 1 μM (greater than 80% inhibition), whereas four compounds (compounds **1**, **8**, **16**, **22**) 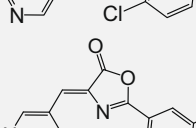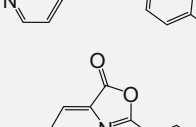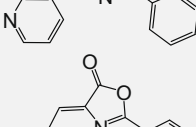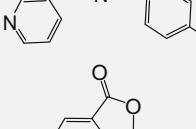had moderately decreased inhibitory activities at 1 μM (less than 80%). Three compounds (compounds **14**, **19**, **20**) had rather weak activities. These results suggest that the inhibitory activity of those compounds depends on the character and position of individual substituted groups.

As shown in Table 3, compound **6** has reduced inhibitory activity at 1 μM, and other compounds selected by the substructure search show no inhibitory activity. Compared to the compounds in Table 2, compound **23** has no activity even at 10 μM, whereas compound **1** shows 95% inhibition at 10 μM. Similar results were appeared in the following compound pairs. Compound **24** and compound **17**; they have the same substituted group (R_2 = Br) on the phenyl ring, compound **25** and compound **15**; R_3 = NO$_2$, and, compound **27** and compound **7**; R_2 = NO$_2$, R_3 = Cl. The compounds in Table 3 (compounds **23**, **24**, **25**, **27**) had significantly reduced inhibitory activities compared to the corresponding compounds in Table 2. This result indicates that Scaffold I is more suitable as the core scaffold than Scaffold II. One possible explanation is that, since the nitrogen atom in the pyridinyl group was predicted to form a hydrogen bond with the backbone NH of Val96 in the hinge region at the ATP binding site (Fig. 2), compounds based on Scaffold I may bind more stably in the ATP binding site than compounds based on Scaffold II. Each of these binding modes is shown in Figure 3; examples of compounds based on Scaffold I are A-1 and A-2, and examples of Scaffold II compounds are B-1 and B-2.

2730

M. Okamoto et al. / Bioorg. Med. Chem. 18 (2010) 2728–2734

Table 1
Results of kinase inhibition assays on compounds selected using a similarity search

Compound	Structure	DAPK3 %inhibition at 10 µM (%)
1 (1st screening hit)		84
2		4
3		45
4		29
5		3
6		97
7		100
8		96
9		96
10		100

2.4. Structure–activity relationships (SARs)

In order to investigate the role of the phenyl ring substituted derivatives, the IC_{50} values of pertinent compounds were determined (Table 4). Of these compounds, compound **17** had the most potent inhibitory activity (IC_{50} = 148 nM). The predicted binding mode of compound **17** at the ATP binding site is shown in Figure 3 (A-1, A-2). The electron density of the phenyl ring and hydrophobic interactions in compound **17** may contribute to making this

substituted phenyl ring the most appropriate ring structure in DAPK inhibitors.

Compound **9** was compared to compound **12**. Both compounds have a chloro substitution but at different positions: *para*-position (R_3; compound **9**) and *meta*-position (R_2; compound **12**). Since the inhibitory activity of compound **12** was more potent than that of compound **9** (IC_{50} values: 360 and 530 nM, respectively), the *meta*-position seems to be more appropriate for binding at the ATP binding site because of electronic effects.

Table 2
Kinase inhibition assay results on compounds selected by a substructure search using the core scaffold, 2-phenyl-4-(3-pyridinylmethylene)-5(4H)-oxazolone (Scaffold I)
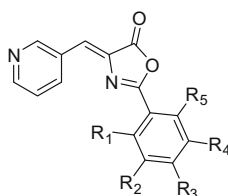
Compound	R$_1$	R$_2$	R$_3$	R$_4$	R$_5$	DAPK3 %inhibition at 10 μM (%)	DAPK3 %inhibition at 1 μM (%)
1	H	H	H	H	H	84	71
7	H	NO$_2$	Cl	H	H	100	100
8	H	CH$_3$	H	H	H	96	68
9	H	H	Cl	H	H	93	85
11	H	F	F	H	H	98	89
12	H	Cl	H	H	H	97	85
13	H	CH$_3$	Br	H	H	94	88
14	H	OCH$_3$	OCH$_3$	OCH$_3$	H	33	26
15	H	H	NO$_2$	H	H	94	90
16	Cl	H	Cl	H	H	78	42
17	H	Br	H	H	H	100	100
18	Br	H	OCH$_3$	H	H	92	100
19	H	Br	OCH$_3$	H	H	32	32
20	H	OCH$_3$	OCH$_3$	H	H	36	14
21	H	OCH$_3$	H	H	H	100	99
22	H	NO$_2$	CH$_3$	H	H	90	72

Table 3
Kinase inhibition assay results on compounds selected by a substructure search using the core scaffold, 2-phenyl-4-(4-pyridinylmethylene)-5(4H)-oxazolone (Scaffold II)
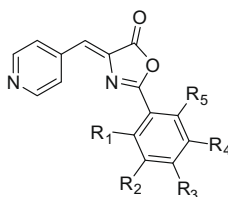
Compound	R$_1$	R$_2$	R$_3$	R$_4$	R$_5$	DAPK3 %inhibition at 10 μM (%)	DAPK3 %inhibition at 1 μM (%)
6	Cl	H	H	I	H	97	83
23	H	H	H	H	H	1	0
24	H	Br	H	H	H	0	1
25	H	H	NO$_2$	H	H	2	0
26	H	NO$_2$	H	H	H	0	0
27	H	NO$_2$	Cl	H	H	10	0

Compound **12** and compound **17** both have one substituted group at the *meta*-position (R$_2$), but the substituted groups are different: a chloro group in compound **12** and a bromo group in compound **17**. Compound **17** has more potent inhibitory activity than compound **12** (IC$_{50}$ values: 148 and 360 nM, respectively), indicating that inhibitory activity is influenced by Br > Cl at the *meta*-position. Another pair of compounds which have one substituted group at the *meta*-position are compound **8** and compound **21**. Compound **21** (R$_2$ = OCH$_3$) has more potent inhibitory activity than compound **8** (R$_2$ = CH$_3$) (IC$_{50}$ values: 395 and 713 nM, respectively). These results indicate that having an electron-withdrawing group at the *meta*-position is very important for potent inhibitory activity by compounds containing a substituted phenyl ring.

The effect of steric repulsion should also be considered. In the predicted binding mode (Fig. 2), the phenyl ring in 2-phenyl-4-(3-pyridinylmethylene)-5(4H)-oxazolone is near Asp161. This area is very tight, so if R$_4$ is a bulky substituted group, the compound may not to be able to bind stably. Compound **14**, which has three methoxy groups (R$_2$, R$_3$, R$_4$ = OCH$_3$), had only weak inhibitory activity even at 10 μM (Table 2), likely due to steric repulsion.

2.5. Kinase selectivity

To study enzyme selectivity, a kinase panel assay was carried out using a ProfilerPro kit (Caliper Life Sciences, Inc., Hopkinton, MA, USA). As shown in Table 5, six compounds in the series appeared to be specific inhibitors of DAPKs (DAPK1, DAPK3). Each compound at 10 μM inhibited DAPK1 and DAPK3, but did not inhibit other serine/threonine- or tyrosine-kinases. This result indicates that compounds containing the 4-(3-pyridinylmethylene)-5(4H)-oxazolone structure have excellent selectivity for DAPKs.

2.6. Calculation of solvated interaction energy (SIE)

In order to better understand the differences in inhibitory activity between compounds based on Scaffold I and Scaffold II, four compound pairs with the same substituted groups were compared regarding ΔG and inhibitory activity, and calculated solvated interaction energy (SIE).[10] SIE can be used to calculate the binding free energy in protein–ligand complexes, and to predict the binding affinity of each ligand.
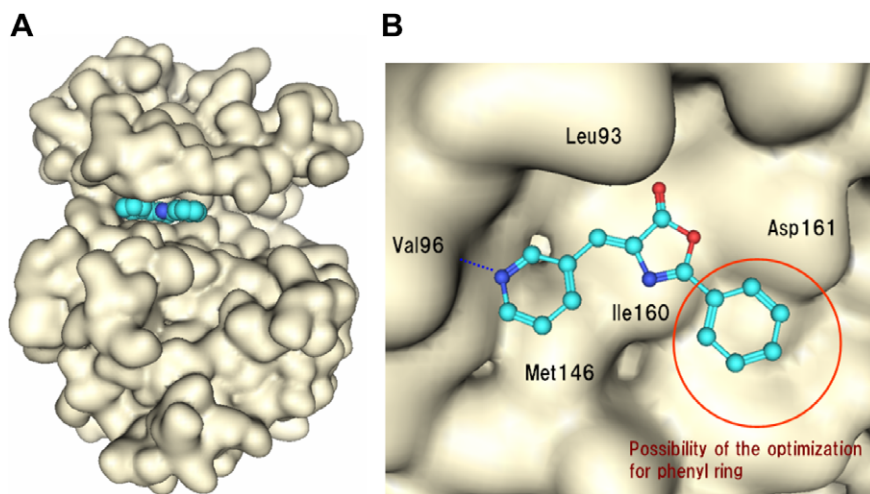
Figure 2. Predicted binding mode of compound **1** to the protein ATP binding site of the protein–ligand complex model. (A) Compound **1** is docked to the DAPK kinase domain. (B) The possibility for structural optimization of the phenyl ring of compound **1** in the ATP binding site. The figure was rendered using MOE.[7]
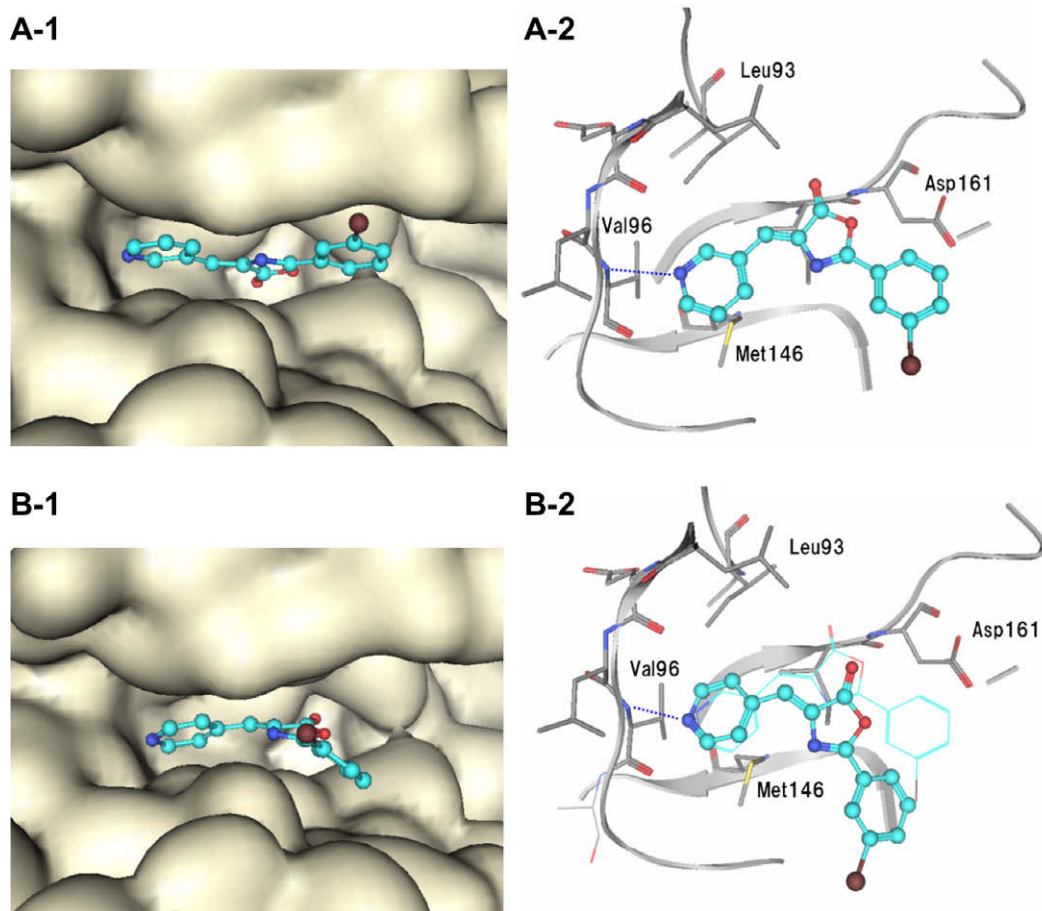
Figure 3. Predicted binding mode of compound **17** and compound **24** in the ATP binding site of DAPK. (A-1) Protein surface and compound **17**. (A-2) Top view of the hydrogen bond between compound **17** and the hinge region of the ATP binding site. (B-1) Protein surface and compound **24**. (B-2) Top view of compound **24** (Ball and Stick) and compound **17** (Line) in the hinge region of the ATP binding site.

As shown in Table 6, the calculated ΔGs appear to correspond to the differences in inhibitory activities of every pair. In every pair, ΔG of the compound based on Scaffold I is better than ΔG of the compound based on Scaffold II. We predicted that compounds with a Scaffold I framework would be able to bind more stably in the ATP binding site than compounds based on Scaffold II because of

Table 4
IC$_{50}$ values of compounds in Tables 1–3 that exhibit significant activity

Compound	R$_1$	R$_2$	R$_3$	R$_4$	R$_5$	IC$_{50}$ (μM)
17	H	Br	H	H	H	0.1484
18	Br	H	OCH$_3$	H	H	0.1570
6[a]	Cl	H	H	I	H	0.2271
13	H	CH$_3$	Br	H	H	0.2529
7	H	NO$_2$	Cl	H	H	0.2785
15	H	H	NO$_2$	H	H	0.2912
11	H	F	F	H	H	0.3461
12	H	Cl	H	H	H	0.3596
21	H	OCH$_3$	H	H	H	0.3953
9	H	H	Cl	H	H	0.5295
22	H	NO$_2$	CH$_3$	H	H	0.5335
1	H	H	H	H	H	0.5830
8	H	CH$_3$	H	H	H	0.7137

[a] The core scaffold is 2-phenyl-4-(4-pyridinylmethylene)-5(4H)-oxazolone (Scaffold II).

Table 5
Kinase selectivity of compounds in the series[a]

Kinase	Compound					
	1	**8**	**9**	**10**	**11**	**13**
DAPK1	98	98	76	91	97	82
DAPK3	95	96	96	100	97	98
MAPKAPK2	5	3	n.d.[b]	46	n.d.	2
AurA	6	3	15	14	8	16
PKCζ	3	2	−3	3	8	5
RSK1	5	15	10	4	n.d.	13
PRAK	n.d.	n.d.	n.d.	5	n.d.	10
Erk1	16	0	25	7	25	18
PKD2	7	1	17	n.d.	3	11
CHK1	3	5	12	12	7	5
ABL	16	1	n.d.	9	n.d.	7
FYN	6	n.d.	n.d.	1	2	9
LYN	10	n.d.	n.d.	1	2	0
CHK2	4	n.d.	24	17	7	19
MET	3	n.d.	n.d.	3	n.d.	n.d.
LCK	9	n.d.	8	8	3	n.d.
SRC	13	5	3	5	6	2
GSK3β	9	n.d.	7	3	0	n.d.
Erk2	7	n.d.	10	20	34	n.d.
PKA	n.d.	n.d.	9	n.d.	2	19
AKT2	13	6	17	17	18	28
INSR	7	3	n.d.	4	7	0
p38α	3	1	2	8	8	5
AKT1	12	5	13	15	12	12
MSK1	n.d.	n.d.	0	13	n.d.	n.d.

[a] The effects of six compounds on the indicated protein kinases were determined using Caliper Life Sciences. Values represent the percent inhibition of each kinase at 10 μM of the test compound.
[b] n.d. = not detected.

Table 6
Calculated solvated interaction energy (SIE)

Compounds pair	Compound	Substituted groups	ΔG	IC$_{50}$
1	**7** (Scaffold I)	R$_2$ = NO$_2$, R$_3$ = Cl	−7.1438	0.2785
	27 (Scaffold II)	R$_2$ = NO$_2$, R$_3$ = Cl	−6.5579	>10
2	**15** (Scaffold I)	R$_3$ = NO$_2$	−6.3972	0.2912
	25 (Scaffold II)	R$_3$ = NO$_2$	−6.0382	>10
3	**17** (Scaffold I)	R$_2$ = Br	−7.0196	0.1484
	24 (Scaffold II)	R$_2$ = Br	−5.9666	>10
4	**1** (Scaffold I)		−5.8907	0.583
	23 (Scaffold II)		−5.6857	>10

their predicted binding mode (2.3.2, Fig. 3). Additionally, the SIE calculations corresponded well to our previous interpretation of the binding mode.

3. Conclusion

After obtaining the first series of hit compounds, a similarity search and a substructure search were used to obtain more potent compounds. The binding mode of the active compounds was predicted using CONSENSUS-DOCK, an in-house docking calculation program, and the structure–activity relationship was analyzed using solvated interaction energy calculations at the ATP binding site. The strategy described in this paper lead to the efficient identification of novel potent DAPK inhibitors. Furthermore, the series of compounds generated during this discovery program showed high selectivity for DAPK, and therefore have potential to contribute to the development of drug treatments for ischemic diseases.

The results described in this paper demonstrate that our in silico approach is very efficient and productive for drug discovery. This strategy will be applicable to other medically important target proteins.

4. Experimental

4.1. Compounds

The database of commercially available compounds was produced by Namiki Shoji Co., Ltd (http://www.namiki-s.co.jp/) and Summit Pharmaceuticals International (SPI; http://www.summit-pharma.co.jp/). The databases include compounds produced by several suppliers. Tested compounds in this paper were purchased from several suppliers (Enamine, ChemDiv, etc.). Their characterizations and purity were confirmed using ^{1}H NMR and HPLC.

4.2. Similarity search

We calculated a fingerprint based on the descriptors of the BIT_MACCS: MACCS structural keys for all compounds in the commercially available databases and conducted a similarity search using MOE[9] with compound **1** as a query. In addition, we selected compounds with appropriate thresholds and by visual inspection, and purchased these compounds from suppliers.

4.3. Substructure search

For compounds selected by the similarity search, we used MDL ISIS™ Base 2.5 SP2 for the substructure search, using the core scaffolds described this article (2.3.2).

4.4. Computational modeling

The predicted binding mode of each compound and the protein structure of the protein–ligand complex model[6] were built using CONSENSUS-DOCK and molecular dynamics (MD) simulation by MOE. In the MD calculations, the system was gradually heated to 300 K, and an additional 1 ns simulation at constant temperature and volume (NVT ensemble, NPA algorithm) was carried out. The equilibrated system was slowly cooled to 0 K and then energy-minimized.

4.5. SIE calculation

Protein–ligand complex models for the SIE calculations were prepared as described above. All the values for ligand–protein interactions and solvation terms were calculated for a single snapshot structure taken after the simulated annealing protocol run. The following equation was used to estimate ligand binding free energies:

$$\Delta G_{bind}(\rho,\ D_{in},\ \alpha,\ \gamma,\ C) = \alpha^{*}[E_{c}(D_{in}) + E_{vdw} + \Delta G^{R}_{bind}(\rho, D_{in})$$
$$+ \gamma \Delta SA(\rho)] + C \qquad (1)$$

where E_{c} and E_{vdw} are the Coulomb and van der Waals terms of interaction energies between ligand and protein. These values were calculated using AMBER FF99 all-hydrogen amino acid parameters for the protein, and general amber force field (GAFF) parameters for the ligands. Partial atomic charges for each ligand were calculated by the semi-empirical AM1-bcc method. ΔG^{R}_{bind} is the difference in the reaction field energy between the bound and unbound states, and were calculated by solving the Poisson equation with the boundary element method.[*] The ΔSA is the difference in the molecular surface area between the complexed and free states. The linear scaling coefficient (ρ), interior dielectric constant (D_{in}), the molecular surface area coefficient (γ), the global proportionality coefficient (α), and a constant (C), were calibrated by fitting to the free energies transferred from the binding or inhibition experimental results for a set of 99 protein–ligand complexes.[9] Optimized values of these parameters were $\rho = 1.1$, $D_{in} = 2.25$, $\gamma = 0.0129$ kcal/mol Å^{2}, $\alpha = 0.1048$, and $C = -2.89$ kcal/mol. The SIE calculations were carried out with these parameter values.

4.6. Kinase assay

The selected compounds were tested in a DAPK3 inhibition assay, and the results are shown in Tables 1–3. The kinase assay was performed using a Z'-LYTE Kinase Assay Kit-Ser/Thr 13 Peptide (Invitrogen, Carlsbad, CA, USA). The standard reaction for compound screening contained 1 mM peptide substrate, 10 μM ATP, 50 mM HEPES (pH 7.4), 10 mM MgCl$_2$, 0.01% Brij-35, and 0.5% DMSO. Human recombinant DAPK3 (Invitrogen) was used at a final concentration 1.5 μg/ml. DAPK1, DAPK3 and ProfilerPro Kits (Caliper Life Sciences, Inc., Hopkinton, MA, USA) were used as described in the protocol to test the enzyme selectively of the inhibitors. Two independent kinase assays were performed to obtain the value of IC$_{50}$. The data represent the average of the duplicate assays. The independent experiments showed results with very close values of IC$_{50}$.

References and notes

1. Deiss, L. P.; Feinstein, E.; Berissi, H.; Cohen, O.; Kimchi, A. *Gene Dev.* **1995**, *9*, 15.
2. Bialik, S.; Kimchi, A. *Annu. Rev. Biochem.* **2006**, *75*, 189.
3. Pelled, D.; Raveh, T.; Riebeling, C.; Fridkin, M.; Berissi, H.; Futerman, A. H.; Kimchi, A. *J. Biol. Chem.* **2002**, *277*, 1957.
4. Shamloo, M.; Soriano, L.; Wieloch, T.; Nikolich, K.; Urfer, R.; Oksenberg, D. *J. Biol. Chem.* **2005**, *280*, 42280.
5. Velentza, A. V.; Wainwright, M. S.; Zasadzki, M.; Mirzoeva, S.; Schumacher, A. M.; Haiech, J.; Focia, P. J.; Egli, M.; Watterson, D. M. *Bioorg. Med. Chem. Lett.* **2003**, *13*, 3465.
6. Okamoto, M.; Takayama, K.; Shimizu, T.; Ishida, K.; Takahashi, O.; Furuya, T. *J. Med. Chem.* **2009**, *52*, 7323.
7. We used databases of commercially available compounds from several suppliers produced by Namiki Shoji Co., Ltd. (http://www.namiki-s.co.jp/) and Summit Pharmaceuticals International (SPI; http://www.summitpharma.co.jp/).
8. MultiCopyMD: we used a molecular dynamics simulation module in MOE[9] by modifying an SVL script to build the complex models. This SVL script was devised to enable several ligand molecules to be positioned in the binding site of the target protein simultaneously during the simulation so that the consensus binding conformation of that protein for multiple ligands can be generated.
9. Molecular Operating Environment (MOE 2006.0801), Chemical Computing Group Inc., 1010 Sherbrooke St. W, Suite 910, Montreal, Quebec, Canada H3A 2R7.
10. Naim, M.; Bhat, S.; Rankin, K. N.; Dennis, S.; Chowdhury, S. F.; Siddiqi, I.; Drabik, P.; Sulea, T.; Bayly, C. I.; Jakalian, A.; Purisima, E. O. *J. Chem. Inf. Model.* **2007**, *47*, 122.